

CLIFFORD TORI AND UNBIASED VECTORS

Ole Andersson¹

Ingemar Bengtsson²

*Fysikum, Stockholms Universitet,
S-106 91 Stockholm, Sweden*

Abstract:

The existence problem for mutually unbiased bases is an unsolved problem in quantum information theory. A related question is whether every pair of bases admits vectors that are unbiased to both. Mathematically this translates to the question whether two Lagrangian Clifford tori intersect, and a body of results exists concerning it. These results are however rather weak from the point of view of the first problem. We make a detailed study of how the intersections behave in the simplest non-trivial case, that of complex projective 2-space (the qutrit), for which the set of pairs of Clifford tori can be usefully parametrized by the unistochastic subset of Birkhoff's polytope. Pairs that do not intersect transversally are located. Some calculations in higher dimensions are included to see which results are special to the qutrit.

Keywords: Mutually unbiased bases, Lagrangian submanifolds, Birkhoff's polytope

¹ole.andersson@fysik.su.se

²ibeng@fysik.su.se

1. Introduction

The existence problem for Mutually Unbiased Bases (MUB) is easy to state, arises naturally when asking questions about the foundations of quantum mechanics, and may have various practical implications [1]. After several decades of work by quantum physicists, it remains open. From a mathematical point of view it is not clear how to address this problem. It just might be bound up with unsolved questions in discrete mathematics such as the existence problem for finite projective planes [2], as has been discussed in the literature [3, 4, 5]. As noticed recently it may also be related to questions in Lagrangian intersection theory, an at first sight unrelated area of mathematics with roots in very different soil [6].

On the physics side the set of all vectors unbiased with respect to a given basis can be regarded as ‘maximally quantum’ states, as seen by an observer having access to only one von Neumann measurement. In mathematics this set of vectors is known as a Clifford torus, and forms a Lagrangian submanifold of complex projective space. Thus, listing the set of all vectors unbiased to two different bases is equivalent to the problem of enumerating the intersections between two Clifford tori. Provided the intersections are transversal (they may not be) a powerful mathematical theorem guarantees that at least 2^{N-1} distinct intersections occur when the Hilbert space has N dimensions [7, 8]. However, to be of use in the MUB existence problem these intersections have to occur in a very special constellation.

The case $N = 2$ is trivial. In this case a Clifford torus is a great circle on the Bloch sphere. Two great circles always intersect in two antipodal points, and these points represent an orthonormal basis unbiased to the two bases one started out with. The purpose of this paper is to investigate the simplest non-trivial case, $N = 3$, in full detail. Using a natural parametrization of the set of all pairs of Clifford tori we find that the number of intersections is 4 or 6, with 3 or 5 intersections occurring in exceptional non-transversal cases.

Section 2 briefly reviews the MUB existence problem and the subject of biunimodular vectors. Section 3 explains why questions about intersecting Lagrangian tori are relevant to it, and recalls some facts about intersecting submanifolds. Section 4 parametrizes the set of Clifford tori by means of the unistochastic subset of Birkhoff’s polytope. A detailed description of the $N = 3$ case is given since it has independent interest. Sections 5 and 6 present our main result, a description of how the regions with four and six intersection points sit inside the parameter space. We pay special attention

to sets of measure zero where the transversality condition fails. Most of the story is based on Mathematica calculations, with some analytical support. We believe that the resulting picture is basically complete—when $N = 3$. The question whether it has any implications for the MUB existence problem is deferred to the concluding section 7. Some analytical calculations for higher dimensions are given in two appendices, to see to what extent our results are special to the $N = 3$ case.

2. The MUB existence problem and biunimodular vectors

In quantum mechanics an orthonormal basis is needed to specify a von Neumann measurement. Given the Hilbert space \mathbf{C}^N , two orthonormal bases $\{|e_i\rangle\}_{i=1}^N$ and $\{|f_i\rangle\}_{i=1}^N$ are said to be *unbiased* if all the numbers $|\langle e_i|f_j\rangle|^2$ are the same. Thus the transition probabilities are

$$p(i|j) = |\langle e_i|f_j\rangle|^2 = \frac{1}{N} \quad (1)$$

for all i, j . Pairs of bases related in this way have practical applications to quantum cryptography, and the concept is closely related to Bohr's notion of complementarity [9], supposedly central to the philosophy of quantum mechanics. One obtains an example of an unbiased pair for any dimension N by letting the first basis be the computational basis, and then acting on its vectors by means of the Fourier matrix F , with matrix elements

$$F_{jk} = \frac{1}{\sqrt{N}} e^{\frac{2\pi i}{N}jk}, \quad 0 \leq j, k \leq N - 1. \quad (2)$$

The resulting basis is called the Fourier basis. Its vectors are made up of the columns of the Fourier matrix.

In the *MUB existence problem* one goes on to ask how many mutually unbiased bases there can be, given N . An answer would have implications ranging from practical quantum state tomography [10, 11] and cryptography [12, 13] to pure mathematics [14]. It is easy to show that the number is bounded from above by $N + 1$. Group theoretical constructions of considerable elegance do yield $N + 1$ mutually unbiased bases in \mathbf{C}^N if the dimension N is a power of a prime number (and yield at least 3 bases in every dimension) [15, 16, 17]. The reason behind this success has been pinpointed [18, 19, 20]. Extensive computer calculations have produced convincing evidence, but no

proof, that the maximum number for $N = 6$ is 3 [21, 22, 23]. Not much more is known about this problem.

A less ambitious problem is that of enumerating the set of all vectors that are unbiased with respect to both members of a pair of unbiased bases. For the particular case that this pair is the computational basis and the Fourier basis, such vectors are also known as biunimodular vectors. They have received considerable attention (also for reasons unrelated to quantum mechanics) [24, 25]. See Table 1, and observe that for $N > 5$ the number of such vectors is larger than one would need in order to construct an additional set of $N - 1$ bases. For $N = 6$ one finds 48 such vectors, and no less than 16 bases can be constructed from them [26]. But there are no unbiased pairs of bases there. This does not settle the MUB existence problem for $N = 6$ as continuous families of unbiased pairs not equivalent to this particular one do exist [27, 28].

Table 1: Number (#) of vectors unbiased to both the computational and Fourier bases in dimension N [24, 25, 26]. If the dimension is divisible by a square the intersection of the two Clifford tori is not transversal.

N	2^{N-1}	$N(N - 1)$	#
2	2	2	2
3	4	6	6
4	8	12	∞
5	16	20	20
6	32	30	48
7	64	42	532

Finally we can ask for all vectors unbiased with respect to an arbitrary, not necessarily unbiased, pair of bases. This is the subject of the next section, albeit in a different language. Again the answer has a practical application to do with error-disturbance relations in quantum theory [29, 30], an observation that inspired this paper. It also has ramifications for the structure of unitary matrices [31, 32]. The paper by Führ and Rzesotnik begins with an up-to-date and very readable review of the subject of biunimodular vectors [32].

3. Clifford tori and their intersections

Quantum states are described, not by vectors in \mathbf{C}^N , but by points in complex projective space \mathbf{CP}^n where $n = N - 1$. This is a Kähler space with a natural metric and a compatible symplectic form. For $N = 3$ an arbitrary point is described, in the computational basis, by the normalized vector

$$\psi = \begin{pmatrix} \sqrt{p_0} \\ \sqrt{p_1} e^{i\nu_1} \\ \sqrt{p_2} e^{i\nu_2} \end{pmatrix}, \quad 0 \leq \nu_1, \nu_2 \leq 2\pi, \quad p_0 + p_1 + p_2 = 1. \quad (3)$$

The vector \vec{p} is a probability vector. If we use the components p_1 and p_2 as two of the coordinates the symplectic form takes the canonical form

$$\Omega = dp_1 \wedge d\nu_1 + dp_2 \wedge d\nu_2. \quad (4)$$

We are now using action-angle coordinates, with the phases ν_i parametrizing tori in phase space [6]. Unitary time evolution is simply Hamiltonian time evolution, for Hamiltonian functions of the special form [33, 34]

$$H(p, \nu) = \langle \psi | \hat{H} | \psi \rangle. \quad (5)$$

If \hat{H} is a diagonal matrix the Hamiltonian function H is independent of the angle variables. In conclusion, complex projective space is a phase space, and unitary transformations are (quite special) canonical transformations.

A torus is *Lagrangian* if it has half the dimension of phase space and if the symplectic form vanishes when restricted to the torus. The action variables p_i parametrize a set of Lagrangian tori that fill the phase space. The metric induced on such a torus is [35]

$$ds^2 = p_1(1 - p_1)d\nu_1^2 + p_2(1 - p_2)d\nu_2^2 - 2p_1p_2d\nu_1d\nu_2. \quad (6)$$

The (metric) area is maximized when the probability vector is flat, that is when

$$p_0 = p_1 = p_2 = \frac{1}{3}. \quad (7)$$

By definition a *Clifford torus* is a Lagrangian torus of maximal area. From the example it is clear that there will be one Clifford torus for each choice of basis in Hilbert space. It is also clear from eq. (1) that a vector is unbiased with respect to a given basis if and only if it corresponds to a point on the Clifford torus defined by that basis.

Mathematicians have devoted considerable attention to the question when two Lagrangian submanifolds, related by a Hamiltonian deformation (in some symplectic manifold), intersect. For the particular case of Clifford tori in complex projective space the result alluded to in the introduction—that the number of distinct intersections is at least 2^n whenever the intersections are transversal—is available [7, 8]. The proofs use sophisticated methods such as Floer cohomology, and we have no intention to comment on them here. We will however need some facts concerning intersecting submanifolds. The dimension of the submanifolds is one half times the (real) dimension of the ambient space.

Consider two circles embedded in a sphere. They are said to *intersect transversally* at a common point if their tangent vectors at this point span the tangent space of the sphere. The sphere has a canonical orientation. If the embedded circles are oriented and ordered we can assign an index $+1$ or -1 to each intersection point depending on whether, at this point, a positively directed tangent vector of the first circle followed by a positively directed tangent vector of the second circle constitute a positively or negatively oriented basis in the tangent space of the sphere. The *intersection number*, I , of the two embedded circles is then defined to be the sum of these indices. One can show that the intersection number is invariant under any smooth deformation of the circles. See e.g. ref. [36]. Now, it is intuitively obvious that the embedded circles can always be deformed so that they do not intersect at all. Therefore $I = 0$, which means that the indices assigned to the transversal intersection points must vanish in oppositely indexed pairs.

The intersection number of two Clifford tori in \mathbf{CP}^n is similarly defined. See section 5. Because it is always possible to smoothly deform the tori so that they do not intersect, their intersection number must equal zero. If, however, we restrict ourselves to Hamiltonian deformations the theorems say that it is impossible to completely separate the Clifford tori—at least 2^n intersection points will stay in the generic case. We will eventually give the calculation of the indices in detail, and we will also be concerned with how they distribute themselves over the MUB intersection points.

Finally we note that, as a glance at Table 1 shows, the theorems we have quoted [7, 8] do not tell the full story. The motivating question is, can they serve as a spring board from which to address the MUB existence problem? The question we will actually address is how things work out in \mathbf{CP}^2 .

4. Birkhoff's polytope

We want to study all possible pairs of Clifford tori in \mathbf{CP}^2 . In this section we will show that up to natural equivalences the set of all such pairs can be parametrized by the four dimensional unistochastic subset of Birkhoff's polytope. An alternative standard form for the matrices connecting the tori is given in Appendix A.

We may assume that the first member of our pair consists of all vectors of the form (3) with a flat \vec{p} . The second member can be obtained by applying a unitary transformation to the first, and the question is where the second torus intersects the first torus. Thus, given a unitary matrix U , we are looking for all choices of phases (α_1, α_2) such that

$$\begin{pmatrix} z_0 \\ z_1 \\ z_2 \end{pmatrix} = U \begin{pmatrix} 1 \\ e^{i\alpha_1} \\ e^{i\alpha_2} \end{pmatrix} \quad \Rightarrow \quad |z_0|^2 = |z_1|^2 = |z_2|^2 = 1 . \quad (8)$$

This gives three, or in the general case N , real equations, but because the matrix is unitary there are in fact only $N - 1$ independent real equations for $N - 1$ unknowns (in dimension N). It is not easy to guess how many solutions there may be.

It is clear that diagonal unitaries D and permutation matrices P transform the computational Clifford torus into itself. For our purposes therefore it is enough to consider equivalence classes of unitaries such that

$$U \sim PDUD'P' . \quad (9)$$

Members of the same equivalence class will give rise to the same number of intersection points. Thus we may present all unitaries in ordered dephased form, meaning that their first row and first column will be filled with non-negative real numbers in non-decreasing order. This equivalence relation arises in many contexts [25]. In practice it is convenient not to impose the permutation equivalences explicitly.

By definition, a *bistochastic* (or doubly stochastic) matrix is a square matrix with positive entries, such that all rows and all columns sum to one. From a unitary matrix we can always construct a bistochastic matrix by taking the Hadamard product $U \circ U^* = B$,

$$U \circ U^* = \begin{bmatrix} |U_{00}|^2 & |U_{01}|^2 & |U_{02}|^2 \\ |U_{10}|^2 & |U_{11}|^2 & |U_{12}|^2 \\ |U_{20}|^2 & |U_{21}|^2 & |U_{22}|^2 \end{bmatrix} = \begin{bmatrix} B_{00} & B_{01} & B_{02} \\ B_{10} & B_{11} & B_{12} \\ B_{20} & B_{21} & B_{22} \end{bmatrix} = B . \quad (10)$$

Bistochastic matrices arising in this way are called *unistochastic*, and they form a proper subset of the set of all bistochastic matrices. If U is an orthogonal matrix B is said to be *orthostochastic*. The set of all dephased unitaries can be parametrized by the independent moduli of the matrix elements. See ref. [37] for a discussion with full references. For $N = 3$ there are 4 parameters, and they determine the dephased unitary uniquely up to complex conjugation, which again is an operation that transforms the computational Clifford torus into itself. For higher values of N this parametrization fails, in principle mildly [38], in practice badly because the unistochastic subset is difficult to characterize.

The set of all bistochastic matrices \mathcal{B} is the convex cover of the permutation matrices, and is called Birkhoff's polytope [39]. The nice thing about this, given that we restrict ourselves to $N = 3$, is that this set is simple enough to be visualized. Visualizing the unistochastic subset \mathcal{U} —which is what we are really interested in—takes a bit more effort, but when $N = 3$ we are greatly helped by the fact that in this case its boundary is easy to characterize: it consists of the set of all orthostochastic matrices, that is the set of bistochastic matrices of the form $B = O \circ O$ where O is an orthogonal matrix. Thus we have an analytic description of the boundary.

Let us give some details (taken from the literature [37]), assuming that we have imposed the Euclidean distance

$$D^2(B_1, B_2) = \frac{1}{2} \text{Tr} \left[(B_1 - B_2)(B_1 - B_2)^T \right] . \quad (11)$$

For any bistochastic matrix B there are permutation matrices P_i and a probability vector $\vec{\pi}$ such that

$$B = \sum_{i=0}^5 \pi_i P_i = \begin{bmatrix} \pi_0 + \pi_1 & \pi_2 + \pi_3 & \pi_4 + \pi_5 \\ \pi_2 + \pi_4 & \pi_0 + \pi_5 & \pi_1 + \pi_3 \\ \pi_3 + \pi_5 & \pi_1 + \pi_4 & \pi_0 + \pi_2 \end{bmatrix} . \quad (12)$$

(Note that this equation provides a labelling of the permutation matrices.) The nine facets of the polytope are obtained by setting one matrix element equal to zero. The polytope is elegantly described as the convex cover of

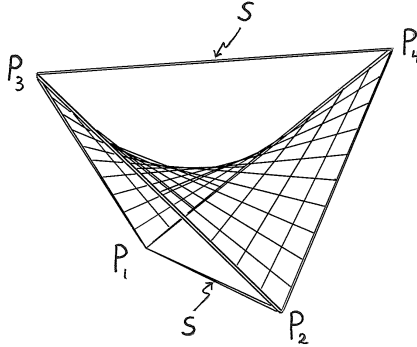


Figure 1: A facet of Birkhoff's polytope. Four edges are unistochastic and bound a ruled surface of unistochastic matrices. Two longer edges are outside the unistochastic set. The matrices at the midpoints of the longer edges are called Schur matrices and are labelled S .

two totally orthogonal regular triangles obtained by setting either $\pi_0 = \pi_3 = \pi_4 = 0$ or $\pi_1 = \pi_2 = \pi_5 = 0$. Its centre of mass sits at the van der Waerden matrix B_\star , a bistochastic matrix with all entries equal. The relative volume of the unistochastic subset is [40]

$$\frac{\text{Vol}[\mathcal{U}]}{\text{Vol}[\mathcal{B}]} = \frac{8\pi^2}{105} \approx 0.752 . \quad (13)$$

Its insphere has radius $r_{\text{in}} = 1/3$, and its outsphere (which coincides with the outsphere of Birkhoff's polytope) has radius 1. Moreover \mathcal{U} is star shaped, i.e. fully visible from its centre.

To see all this in front of us, we begin by looking at a facet of Birkhoff's polytope. It is a tetrahedron with four edges of length $\sqrt{2}$ and two edges of length $\sqrt{3}$. The unistochastic subset meets the facet in a two dimensional ruled surface, coming from a maximal torus in the group manifold of $SO(3)$. The short edges are unistochastic, the long ones not. See Fig. 1.

Next we look at a selection of cross sections through the polytope. First we take the cross section $\pi_1 = \pi_2 = \pi_5 = 0$. This is an equilateral triangle bounded by three non-unistochastic edges, and the polytope itself is the convex cover of two such triangles. The curve bounding the unistochastic subset is known as a deltoid. The three points on this curve closest to the centre lie on the insphere of the unistochastic subset. See Fig. 2.

Moving somewhat beyond ref. [37], we also look at cross sections obtained

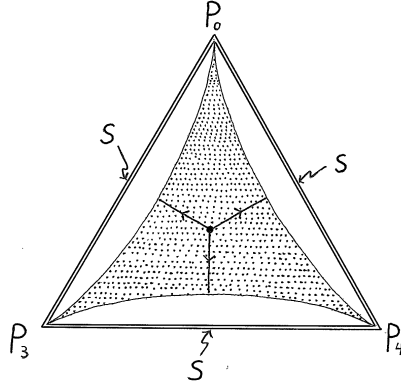


Figure 2: A cross section through Birkhoff's polytope, centred at the van der Waerden matrix and including three non-unistochastic edges. The unistochastic subset (shaded) is bounded by a hypocycloid (covering unitaries with exceptional properties—see Section 6). Its insphere touches this boundary right below the Schur matrices (S). The paths emerging from the centre reappear as paths “b” in Fig. 6. Birkhoff's polytope is the convex cover of two totally orthogonal triangles of this type.

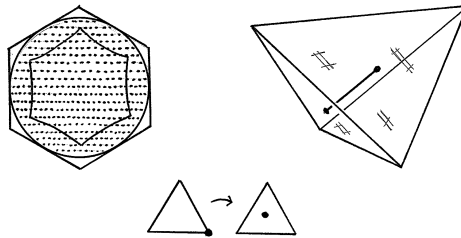


Figure 3: A hexagonal cross section. Its edges lie in facets, as shown on the right, with its corners at midpoints of faces. The unistochastic subset (shaded) is bounded by a circle, and its interior is divided into two regions by a boundary to be discussed in section 6.

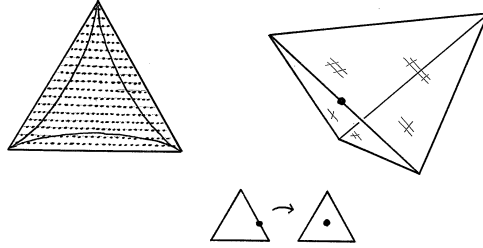


Figure 4: A triangular cross section, consisting entirely of unistochastic matrices. Its corners lie at midpoints of unistochastic edges in the facets, as shown on the right. The cross section is divided into two regions by a hypocycloid, as discussed in section 6.

by taking all bistochastic matrices such that $B\vec{p} = \vec{e}$, where \vec{p} is some fixed probability vector and \vec{e} is the flat probability vector. Generically they are hexagons. A case where the hexagon is regular is shown in Fig. 3. Its unistochastic subset is a circular disk. A case where the hexagon degenerates to an equilateral triangle is shown in Fig. 4. It lies entirely within the unistochastic subset. In both pictures the unistochastic subset is divided into two regions, for reasons that will become clear in section 6.

A fourth cross section is obtained by including B_\star and a unistochastic edge. The boundary of its unistochastic subset is a parabola. The bisectrices of the triangles making up the first kind of cross section occur as diagonals in these parabolic cross sections. See Fig. 6 (which is placed in section 6 because we will provide more details there).

5. Intersections—at the extremes

We consider pairs of Clifford tori related by a unitary matrix according to eq. (8). Using the parametrization of the pairs given in section 4 we begin with pairs whose parameterizing unitaries sit inside a facet of Birkhoff's polytope.

In each facet these unitaries make up a two dimensional set of orthogonal matrices, and it is easy to verify analytically that they relate tori intersecting in exactly 4 points, with the exception of those matrices that sit on an edge of the polytope [32]. The latter relate tori that intersect non-transversally in two non-intersecting circles. For an example see panel “d” in Fig. 7. If the matrix is a permutation matrix the tori coincide.

Then we venture inside, and choose the unitary to equal the Fourier matrix F ,

$$F = \frac{1}{\sqrt{3}} \begin{pmatrix} 1 & 1 & 1 \\ 1 & \omega & \omega^2 \\ 1 & \omega^2 & \omega \end{pmatrix}, \quad \omega = e^{\frac{2\pi i}{3}}. \quad (14)$$

Its columns form the Fourier basis. The corresponding bistochastic matrix is the van der Waerden matrix, and sits at the centre of Birkhoff’s polytope. It is known that the computational and Fourier basis can be supplemented with two additional bases to form a complete set of four mutually unbiased bases [10]. This means that there exist (at least—and in fact exactly) six vectors unbiased to both, and hence the two Clifford tori intersect in six points. The intersections are transversal, meaning that the 2-dimensional tangent spaces of the two tori span the 4-real-dimensional tangent space of the ambient space at the intersections. A special feature is that the vectors in the Fourier basis sit in the computational Clifford torus. Conversely the computational basis vectors sit in the Clifford torus defined by the Fourier basis.

Now a torus is an orientable manifold, and \mathbf{CP}^2 is oriented by the choice of the symplectic form. Following section 3 we can assign an index ± 1 to each point where the tori intersect transversally. We permit ourselves to use some standard notation from differential geometry, where tangent vectors appear as differential operators. We use affine coordinates for the calculation (which is given in more detail in the appendix). Vectors in Hilbert space are written as $(1, z_1, z_2)$. The first Clifford torus is described by $(z_1, z_2) = (e^{i\nu_1}, e^{i\nu_2})$, and its tangent spaces are spanned by the vector fields

$$\partial_{\nu_1} = iz_1 \partial_{z_1} - i\bar{z}_1 \partial_{\bar{z}_1} \quad \partial_{\nu_2} = iz_2 \partial_{z_2} - i\bar{z}_2 \partial_{\bar{z}_2}, \quad (15)$$

which are the pushforwards of the coordinate vector fields of (ν_1, ν_2) , computed by the chain rule. The second torus is related to the first by the Fourier matrix, and its embedding is defined by

$$\begin{pmatrix} 1 \\ z_1(\alpha_1, \alpha_2) \\ z_2(\alpha_1, \alpha_2) \end{pmatrix} \sim \frac{1}{\sqrt{3}} \begin{pmatrix} 1 & 1 & 1 \\ 1 & \omega & \omega^2 \\ 1 & \omega^2 & \omega \end{pmatrix} \begin{pmatrix} 1 \\ e^{i\alpha_1} \\ e^{i\alpha_2} \end{pmatrix}. \quad (16)$$

The \sim symbol means equality up to an overall complex number. In this way we obtain a parametric description of the second torus. Finally we calculate the pushforwards of the coordinate vector fields under (16), and call them $\partial_{\alpha_1}, \partial_{\alpha_2}$. We then have bases in the tangent spaces of the tori, which we declare to be orientation determining. The tori intersect at the six points

$$\begin{pmatrix} z_1 \\ z_2 \end{pmatrix} = \begin{bmatrix} \omega^2 & 1 & \omega & \omega & \omega^2 & 1 \\ \omega^2 & \omega & 1 & \omega & 1 & \omega^2 \end{bmatrix}. \quad (17)$$

Our altogether four tangent vector fields span the tangent spaces of \mathbf{CP}^2 at these points, and we can calculate the orientation of the bases there. The end result of this somewhat lengthy calculation is that

$$\det \left[\partial_{\nu_1} \quad \partial_{\nu_2} \quad \partial_{\alpha_1} \quad \partial_{\alpha_2} \right] = \pm 3, \quad (18)$$

with the plus sign occurring three times and the minus sign three times. Thus the intersection number $I = 0$, as advertized in section 3. But the calculation also gives an index associated to each of the intersections, and therefore also some information about how the intersection points can merge, or not, as we deform the tori. Interestingly the signs are all plus for a triplet of points corresponding to one basis, and all negative for the other. See Fig. 5. The question whether this pattern repeats itself in all odd prime dimensions is addressed in appendix B.

If we move the second torus by means of a continuous family of unitary transformations the location of the intersection points will change, and they may even merge and disappear. But the sum of the indices of the intersection points will be preserved during this process, and this restricts the pattern of possible mergers. We know what goes on at the boundary and at the centre of our parameter space. Except for a set of measure zero the boundary consists of unitaries that give rise to only 4 intersection points. In an open ball around the centre 6 intersection points arise. Somewhere in between must lie a boundary between those unitaries relating tori that intersect 4 times, and those relating tori intersecting 6 times. The aim of the next section is to pin this boundary down.

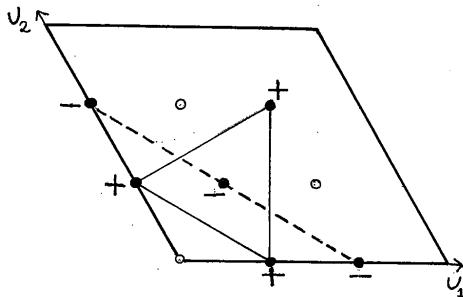


Figure 5: The computational Clifford torus is drawn with its correct shape as given by eq. (6). Opposite sides are identified. The 6 points where this torus is intersected by a second torus, related to the first by the Fourier matrix, are shown with their indices. They form two bases, as indicated (due to the periodicity the dashed line is another triangle in disguise). The four bases involved in this construction form a complete set of MUB.

6. How the intersections move and merge

We want a precise account of how the intersections change as we vary the pairs of tori. We begin by looking at pairs related by a matrix picked from the cross section in Fig. 6. Four paths from its centre to its boundary are drawn and labelled. At the starting point (the Fourier matrix) there are 6 intersections, supplied with indices according to Fig. 5. The motion of the intersection points is shown in Fig. 7. As we move along the path labelled “a” a pair of intersections merge and disappear when we cross the part of the inner boundary marked “5” in the picture. The remaining 4 intersections continue to move until we hit the boundary of the unistochastic set. Along path “b” the number of distinct intersections stays 6 all the way to the corner, where it drops to 3. Along path “c” three intersections merge when we reach the inner boundary marked “4” in the picture. On the other side of this boundary the number of intersections is 4. Along path “d” the number of intersections remains 6 all the way to the unistochastic edge, where the intersections form two circles. The behaviour is qualitatively the same for all paths from the centre, the one thing that matters is which part of the boundary—“5”, “4”, or neither—that is being crossed.

Inspection of Fig. 7b suggests that it may be possible to continuously and unitarily move the Clifford torus of the Fourier basis into coincidence with that of the computational basis in such a way that three intersection

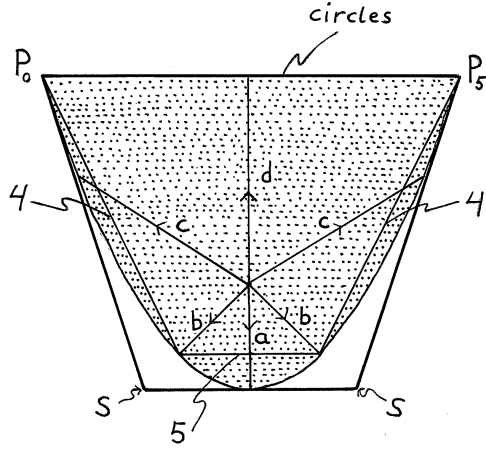


Figure 6: A cross section including a unistochastic edge and the van der Waerden matrix. The unistochastic subset is bounded by a parabola. The region where six intersections occur is bounded by an inner boundary consisting of straight lines. On these the number of intersections drops to either 4 or 5, as indicated by the respective labels. Notice the six paths (of four types) from the van der Waerden matrix to the boundary. They are displayed in a different way in Fig. 7. Paths of type “b” also appear in Fig. 2.

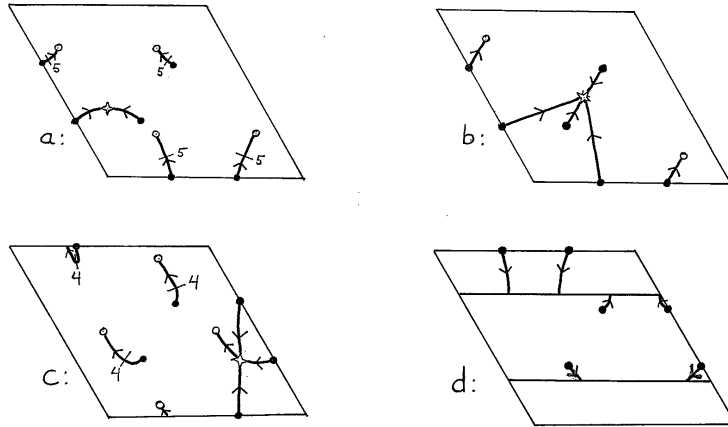


Figure 7: How the intersections points move and merge as we change the matrix from Fourier to the boundary along the four different paths shown in Fig. 6. In case b (also shown in Fig. 2) one of the bases remains a basis all along the path—and it could have been kept fixed, see Appendix A. In case d we approach a pair of Clifford tori intersecting in two circles. The behaviour is ruled by the indices assigned in Fig. 5, and the coordinates used are the α_i from eq. (8).

points (belonging to a single basis) remain fixed. We prove this, and sketch the corresponding proof for N intersection points in all odd prime dimensions N , in Appendix A. For $N = 2$ a look at the Bloch sphere suffices as a proof.

The full picture is drawn with limited analytical support. Using Mathematica we checked a fairly large number of paths, until we were confident about the analytic form of the inner boundary. Then we checked numerically that matrices along this inner boundary behave as expected, and finally we calculated the intersections analytically in a few examples.

Which of these behaviours is typical? To answer this question we repeated the exercise for the other three cross sections we have studied. In the example shown in Fig 3 the cross section is cleanly divided into two regions with 6 intersections in the central region, 4 intersections in the exterior region, and 5 intersections along the boundary. In Fig. 4 the behaviour is similar, except if the path escapes at the corners where the intersections grow into two circles. There are 5 intersections along the inner boundary, which forms a hypocycloid. The cross section shown in Fig. 2 is a very special case. In this case there are 6 intersections throughout the interior, and their number drops to 3 all along its boundary (except, of course, at the corners). This is not in contradiction to the theorems [7, 8] since the intersections cease to be transversal there.

Thus pairs of Clifford tori that intersect in only 3 distinct points occur at the boundary of the unistochastic set in the two special cross sections shown in Fig. 2. Incidentally, the path “b” from Fig. 6 lies along a bisectrix in Fig. 2. This gives us a useful double check on the neighbourhood of the interesting matrix encountered at the boundary there. For this very symmetrical choice of path one of the bases formed by the intersection points moves as a unit, and remains a basis all along the path. The paths “a” and “d” lie along a bisectrix in Fig. 4 and provide a double check on the behaviour at the unistochastic edge.

One of our aims was to find an analytic description of the boundary separating regions of matrices giving rise to Clifford tori with 6 and 4 intersections, respectively. In this we failed, but the cross sections we have shown give much information about its shape. They suggest, as expected, that the boundary between the two regions generically consists of matrices with 5 cross sections, although exceptions were identified. They support the conjecture that the region giving rise to 6 intersections is star shaped. In looking at the pictures we should remember that Birkhoff’s polytope lives in four dimensions, and most of its volume lies far from its centre. When we

Table 2: Number of randomly generated unitary matrices relating Clifford tori with $\#$ intersections (out of 10^5 examples in dimensions 3 and 4).

Dimension 3	$\# = 4$	$\# = 6$			
	80 591	19 409			
Dimension 4	$\# = 8$	$\# = 10$	$\# = 12$	$\# = 14$	$\# = 16$
	31 882	44 425	22 023	1 605	65

picked unitary matrices at random using the Haar measure we found that the region giving rise to 6 intersections occurs about one fifth of the time (as has been independently confirmed [41]). The average Euclidean distance from the centre of Birkhoff's polytope was 0.49 for matrices leading to 4 intersections, and 0.37 for those leading to 6 intersections. Table 2 gives precise results. For each matrix generated we solved eq. (8) numerically to 60 digits precision. The exercise was then repeated for $N = 4$ dimensions in order to see if the lowest possible number of intersections is always the most common case. It is not.

7. Discussion

In conclusion, Clifford tori in \mathbf{CP}^1 always intersect in two points. The first non-trivial case occurs in \mathbf{CP}^2 . In this case generic pairs of Clifford tori intersect in either 4 or 6 points, the former case having the largest Haar measure. (In four dimensions the largest measure pertains to Clifford tori intersecting more than the 2^3 times guaranteed by the theorems [7, 8].) We observed that pairs of Clifford tori can be parametrized, up to natural equivalences, by the unistochastic subset \mathcal{U} of Birkhoff's polytope, which in this case is a four dimensional set whose structure is well understood. This set is divided into two regions. The region corresponding to 6 intersections contains the centre of \mathcal{U} , while the closure of the region corresponding to 4 intersections contains the boundary of \mathcal{U} . On the boundary between these regions one typically but not always finds 5 distinct intersections. Clifford tori intersecting in only 3 points occur along two distinct curves in the set of inequivalent pairs, namely on the boundary of the unistochastic set in the two special cross sections depicted in Fig. 2.

We described the situation by giving a precise account of four different two dimensional cross sections of \mathcal{U} . Based on them we conjecture that the region corresponding to 6 intersections is star shaped, and that pairs intersecting in just 3 distinct points occur only along the two curves we identified.

The intersection number for a pair of Clifford tori vanishes, but the individual signs distribute themselves in an interesting way when there are six intersection points corresponding to a MUB: the signs are all plus for one basis, and all negative for the other. This pattern recurs in (at least) all odd prime dimensions ≤ 17 , so this is not an $N = 3$ coincidence. It is connected to the fact that the MUB vectors fall in two groups, depending on whether their components can be constructed from the root of unity $e^{2\pi i/N}$ raised to quadratic residues or quadratic non-residues.

Now the question is whether we have learned anything of use for the MUB existence problem? In Figs. 2 and 6 the arrows clearly go the “wrong” way. The calculations were performed along curves starting at the Fourier case and moving outwards towards the boundary of the set. What we would really like to do is to set up some kind of natural flow in the set of pairs of Clifford tori, such that the intersection pattern changes towards the pattern that signals the presence of a complete set of MUBs. In dimensions where the MUB existence problem has a negative answer, obstructions to this flow should be identified. Whether anything like this can be achieved we do not know.

It will occur to the reader that, since we restricted ourselves to the lowest non-trivial dimension, our pictures do not even begin to capture the complexities hidden behind Table 1. This is true. Of course there are contexts in which the qutrit, or \mathbf{CP}^2 , is of special interest. Moreover, the geometry of the unistochastic subset of 3 by 3 bistochastic matrices is of independent interest [42]. Nevertheless, our purpose was to inject new ideas that may lead to progress in all dimensions, and we hope they will.

Acknowledgements

We thank Karol Życzkowski for drawing our attention to Cho’s work, Zbigniew Puchała for sending nice pictures, and David Andersson for technical help.

Appendix A: Some calculations in higher dimensions

We have characterized pairs of Clifford tori by the unitary matrices connecting them, and we divided the latter into equivalence classes, choosing a dephased unitary as representing each class. This is very convenient in 3 dimensions, but in higher dimensions an alternative standard form may be preferable. Given the theorems on which we rely [7, 8] we know that every Clifford torus intersects the computational Clifford torus, and by translations along the tori (that is, by enphasizing the unitary that connects them) we can ensure that one of the intersection points is represented by the flat vector (all of whose entries are equal to $1/\sqrt{N}$). Denote this vector by $|f_0\rangle$, and extend it to an orthonormal basis $\{|f_i\rangle\}_{i=0}^{N-1}$ in some way. Then each equivalence class has a representative unitary matrix of the form

$$U = |f_0\rangle\langle f_0| + \sum_{i=1}^{N-1} e^{i\sigma_i} |f_i\rangle\langle f_i|. \quad (19)$$

By construction, the flat vector is left invariant by this matrix. There are $(N-1)(N-2)$ real parameters involved in the choice of the basis and $N-1$ parameters in the eigenvalues, so the dimension of the set of inequivalent pairs of Clifford tori is $(N-1)^2$, which is equal to the dimension of Birkhoff's polytope.

We can now give an example of a one-parameter family of unitaries $U(\sigma)$, $\sigma \in [0, \pi]$, interpolating between the identity and a matrix in the same equivalence class as the Fourier matrix F , and which relates Clifford tori that intersect at the vectors in the Fourier basis for all values of the parameter. The matrix elements are

$$U_{uv}(\sigma) = \frac{1}{N} \sum_{s=0}^{N-1} e^{i\sigma s^2} \omega^{(u-v)s}, \quad 0 \leq u, v \leq N-1, \quad \omega = e^{\frac{2\pi i}{N}}. \quad (20)$$

This substantiates the claim made in section 5, namely that in all prime dimensions it is possible to continuously and unitarily move the standard torus into coincidence with the Fourier torus in such a way that N intersection points, forming one of the bases in a MUB, are left fixed.

The proof uses a standard Gauss sum valid for odd prime N , eq. (32) below. However, the idea becomes much more transparent if we write it out for $N=3$, in which case the one-parameter family is given by

$$U(\sigma) = \frac{1}{3} \begin{pmatrix} 1 \\ 1 \\ 1 \end{pmatrix} (1 \ 1 \ 1) + \frac{e^{i\sigma}}{3} \begin{pmatrix} 1 \\ \omega \\ \omega^2 \end{pmatrix} (1 \ \omega^2 \ \omega) + \frac{e^{i\sigma}}{3} \begin{pmatrix} 1 \\ \omega^2 \\ \omega \end{pmatrix} (1 \ \omega \ \omega^2) . \quad (21)$$

For $\sigma = 0$ this gives the identity, for $\sigma = 2\pi/3$ it covers the van der Waerden matrix, and for $\sigma = \pi$ it reaches the boundary of the unistochastic set. The six intersection points of the tori related by this matrix are given by vectors $(1, e^{i\alpha_1}, e^{i\alpha_2})$ equal to one of the columns of the matrix

$$\begin{bmatrix} 1 & 1 & 1 & 1 & 1 & 1 \\ 1 & \omega & \omega^2 & -e^{ia} & -e^{ia} & 1 \\ 1 & \omega^2 & \omega & -e^{ia} & 1 & -e^{-ia} \end{bmatrix} , \quad (22)$$

where

$$e^{ia} = \frac{1 + 2e^{i\sigma}}{2 + e^{i\sigma}} . \quad (23)$$

This provides an analytic check on Fig. 7b, although in that picture the “fixed basis” moves because we used a different standard form of the unitaries. (By the way, our figures rely not only on numerical calculations but also on quite a few analytic checks of this kind.)

Appendix B: Calculating the intersection indices

We will now calculate the intersection indices, in odd prime dimensions, for a pair of Clifford tori related by the Fourier matrix F . In general odd prime dimensions p a complete set of MUB can be taken to consist of the computational basis, the Fourier basis, and $p - 1$ bases given by columns of circulant matrices [10]. Let the non-zero integer $z < p$ label the circulant bases and the integer $a < p$ label the vectors. With $\omega = e^{2\pi i/p}$ and using arithmetic modulo p whenever applicable, we have the MUB vectors

$$|z, a\rangle \sim \sum_{r=0}^{p-1} \omega^{\frac{(r-a)^2}{2z}} |e_r\rangle \sim \sum_{r=0}^{p-1} \omega^{\frac{r^2 - 2ra}{2z}} |e_r\rangle , \quad (24)$$

where we removed a phase factor in the last step in order to prepare for using affine coordinates. When we apply the discrete Fourier transformation the vectors are rearranged according to

$$|z, a\rangle \rightarrow |z', a'\rangle = \left| -\frac{1}{z}, \frac{a}{z} \right\rangle . \quad (25)$$

We use the angles ν_r to coordinatize the fixed torus and the angles α_r to coordinatize the torus that we shift with the Fourier matrix. At the intersection points defined by these vectors, see eq. (24), we have then that

$$e^{i\alpha_r} = \omega^{\frac{r^2-2ra}{2z}} \quad \Rightarrow \quad z_r = e^{i\nu_r} = \omega^{-\frac{zr^2}{2}+ra} . \quad (26)$$

This gives the affine coordinates z_r evaluated at these intersection points. A general point on the shifted torus ends up at

$$z_r = z_r(\alpha) = \frac{\sum_{s=0}^{p-1} \omega^{rs} e^{i\alpha_s}}{\sum_{s=0}^{p-1} e^{i\alpha_s}} \quad \Rightarrow \quad \frac{\partial z_s}{\partial \alpha_r} = i e^{i\alpha_r} \frac{\omega^{sr} - z_s}{\sum_s e^{i\alpha_s}} . \quad (27)$$

Finally we can write down the tangent vectors of the two tori at the intersection points, namely

$$\partial_{\nu_r} = i z_r \partial_{z_r} - i \bar{z}_r \partial_{\bar{z}_r} \quad (28)$$

$$\partial_{\alpha_r} = \sum_{s=0}^{p-1} \left(\frac{\partial z_s}{\partial \alpha_r} \partial_{z_r} + \frac{\partial \bar{z}_s}{\partial \alpha_r} \partial_{\bar{z}_r} \right) , \quad (29)$$

where the premise in (26) is assumed to hold.

Unfortunately we were unable to calculate the resulting determinant in general. For $p = 3, 7, 11$ we found

$$\det[\partial_{\nu_1}, \dots, \partial_{\nu_{p-1}}, \partial_{\alpha_1}, \dots, \partial_{\alpha_{p-1}}] = \pm p , \quad (30)$$

where the plus sign applies to all vectors coming from a basis $|z, a\rangle$ with z a quadratic residue. For $p = 5, 13, 17$ it is again true that the determinant is positive for all vectors coming from a basis whose z is a quadratic residue, but for these three cases we found respectively that

$$\det = \frac{5}{2}(\pm 3 - \sqrt{5}) , \quad \det = \frac{13}{2}(\pm 11 - 3\sqrt{13}) , \quad \det = 17(\pm 33 - 8\sqrt{17}) . \quad (31)$$

The difference between primes equal to 3 modulo 4 and primes equal to 1 modulo 4 is due to the Gauss sum

$$\sum_{x=0}^{p-1} \omega^{x^2} = 1 + 2 \sum_{x \in \mathbf{Q}} \omega^x = \begin{cases} \sqrt{p} & \text{if } p = 4k + 1 \\ i\sqrt{p} & \text{if } p = 4k + 3, \end{cases} \quad (32)$$

where \mathbf{Q} denotes the set of quadratic residues (i.e., the set of non-negative integers that can be written as the square of another integer in arithmetic modulo p). Sums over roots of unity with quadratic (non-)residues are easily calculated from this formula.

The conclusion is that we have some evidence for the conjecture that the intersection indices are always equal for intersection points taken from the same mutually unbiased basis if the dimension is an odd prime—but we did not prove it.

References

- [1] T. Durt, B.-G. Englert, I. Bengtsson, and K. Życzkowski, *On mutually unbiased bases*, Int. J. Quantum Inf. **08**, 535, 2010.
- [2] C. W. H. Lam, *The search for a finite projective plane of order 10*, Amer. Math. Mon. **98**, 305, 1991.
- [3] T. Paterek, M. Pawłowski, M. Grassl and Č. Brukner, *On the connection between mutually unbiased bases and orthogonal Latin squares*, Phys. Scr. **2010**, 014031, 2010.
- [4] S. Weigert and T. Durt, *Affine constellations without mutually unbiased counterparts*, J. Phys. A: Math. Theor. **43**, 402002, 2010.
- [5] M. Weiner, *A gap for the maximum number of mutually unbiased bases*, Proc. Amer. Math. Soc. **141**, 1963, 2013.
- [6] V. I. Arnold: *Mathematical methods in classical mechanics*, Springer, New York 1989.
- [7] P. Biran, M. Entov, and L. Polterovich, *Calabi quasimorphisms for symplectic ball*, Commun. Contemp. Math. **06**, 793, 2004.
- [8] C. H. Cho, *Holomorphic disks, spin structures and Floer cohomology of the Clifford torus*, Int. Math. Res. Not. **2004** 1803.
- [9] J. Schwinger: *Quantum Mechanics. Symbolism of Atomic Measurements*, ed. by B.-G. Englert, Springer, Berlin 2001.

- [10] I. D. Ivanović, *Geometrical description of state determination*, *J. Phys.* **A14**, 3241, 1981.
- [11] W. K. Wootters, *A Wigner-function formulation of finite-state quantum mechanics*, *Ann. Phys.* **176**, 1, 1987.
- [12] N. J. Cerf, M. Bourennane, A. Karlsson, and N. Gisin, *Security of quantum key distribution using d-level systems*, *Phys. Rev. Lett.* **88**, 127902, 2002.
- [13] M. Mafu et al., *Higher-dimensional orbital angular momentum based quantum key distribution with mutually unbiased bases*, *Phys. Rev.* **A88**, 032305, 2013.
- [14] A. I. Kostrikin and P. I. Tiep: *Orthogonal decompositions and integral lattices*, de Gruyter, Berlin 1994.
- [15] W. K. Wootters and B. D. Fields, *Optimal state-determination by mutually unbiased bases*, *Ann. Phys. NY* **191**, 363, 1989.
- [16] C. Godsil and A. Roy, *Equiangular lines, mutually unbiased bases, and spin models*, *Eur. J. Comb.* **30**, 246, 2009.
- [17] W. M. Kantor, *MUBs inequivalence and affine planes*, *J. Math. Phys.* **53**, 032204, 2012.
- [18] S. Bandyopadhyay, P. O. Boykin, V. Roychowdhury and F. Vatan, *A new proof for the existence of mutually unbiased bases*, *Algorithmica* **34**, 512, 2002.
- [19] M. Aschbacher, A. M. Childs, and P. Wocjan, *The limitations of nice mutually unbiased bases*, *J. Algebra. Comb.* **25**, 111, 2007.
- [20] H. Zhu, *Mutually unbiased bases as minimal Clifford covariant 2-designs*, *Phys. Rev.* **A91**, 060301, 2015.
- [21] S. Brierley and S. Weigert, *Maximal sets of mutually unbiased quantum states in dimension six*, *Phys. Rev.* **A78**, 04312, 2008.
- [22] P. Jaming, M. Matolcsi, P. Móra, F. Szöllösi, and M. Weiner, *A generalized Pauli problem and an infinite family of MUB-triplets in dimension 6*, *J. Phys.* **A42**, 245305, 2009.
- [23] P. Raynal, X. Lü, and B.-G. Englert, *Mutually unbiased bases in dimension six: The four most distant bases*, *Phys. Rev.* **A83**, 062303, 2011.
- [24] G. Björck and B. Saffari, *New classes of finite unimodular sequences with unimodular Fourier transforms*, *C. R. Acad. Sci., Paris, Sér. I* **320**, 319, 1995.

- [25] U. Haagerup, *Orthogonal maximal abelian *-subalgebras of the $n \times n$ matrices and cyclic n -roots*, in *Operator Algebras and Quantum Field Theory, Rome (1996)*, Internat. Press, Cambridge, MA 1997.
- [26] M. Grassl, *On SIC-POVMs and MUBs in dimension 6*, arXiv eprint quant-ph/0406175.
- [27] B. R. Karlsson, *Three-parameter complex Hadamard matrices of order 6*, *Lin. Alg. Appl.* **434**, 247, 2011.
- [28] F. Szöllösi, *Complex Hadamard matrices of order 6: a four-parameter family*, *J. London Math. Soc.* **85**, 616, 2012.
- [29] K. Korzekwa, D. Jennings, and T. Rudolph, *Operational constraints on state-dependent formulations of quantum error-disturbance trade-off relations*, *Phys. Rev* **A89**, 052108, 2014.
- [30] Z. Puchała, Ł. Rudnicki, K. Chabuda, M. Paraniak, and K. Życzkowski, *Certainty relations, mutual entanglement and non-displacable manifolds*, *Phys. Rev.* **A92**, 012304, 2015.
- [31] M. Idel and M. M. Wolf, *Sinkhorn normal form for unitary matrices*, *Lin. Alg. Appl.* **471**, 76, 2015.
- [32] H. Führ and Z. Rzeszotnik, *On biunimodular vectors for unitary matrices*, *Lin. Alg. Appl.* **484**, 86, 2015.
- [33] T. W. B. Kibble, *Geometrization of quantum mechanics*, *Commun. Math. Phys.* **65**, 189, 1979.
- [34] D. C. Brody and L. P. Hughston, *Geometric quantum mechanics*, *J. Geom. Phys.* **38**, 19, 2001.
- [35] I. Bengtsson and K. Życzkowski: *Geometry of Quantum States*, Cambridge University Press, Cambridge, 2006
- [36] V. Guillemin and A. Pollack: *Differential Topology*, Prentice-Hall, New Jersey 1974.
- [37] I. Bengtsson, Å. Ericsson, M. Kuś, W. Tadej, and K. Życzkowski, *Birkhoff's polytope and unistochastic matrices, $N = 3$ and $N = 4$* , *Commun. Math. Phys.* **259**, 307, 2005.
- [38] A. V. Karabegov, *A mapping from the unitary to the doubly stochastic matrices and symbols on a finite set*, *AIP Conf. Proc.* **1079**, 39, 2008.

- [39] G. Birkhoff, *Tres observaciones sobre el algebra lineal*, Univ. Nac. Tucumán Rev. **A5**, 147, 1946.
- [40] C. Dunkl and K. Życzkowski, *Volume of the set of unistochastic matrices of order 3 and the mean Jarlskog invariant*, J. Math. Phys. **50**, 123521, 2009.
- [41] Z. Puchała, private communication.
- [42] G. W. Gibbons, S. Gielen, C. N. Pope, and N. Turok, *Measures on mixing angles*, Phys. Rev. **D79**, 013009, 2009.

